Minireview

Defining the radiobiology of prostate cancer progression: An important question in translational prostate cancer research

Srinivas Vourganti[1], Jeffrey Donaldson[1], Linda Johnson[3], Baris Turkbey[3], Gennady Bratslavsky[1] and Leszek Kotula[1,2]

[1]Department of Urology, SUNY Upstate Medical University, Syracuse, NY 13210, USA; [2]Department of Biochemistry and Molecular Biology, SUNY Upstate Medical University, Syracuse, NY 13210, USA; [3]Molecular Imaging Program, Urologic Branch, National Cancer Institute, National Institutes of Health, Bethesda, MD 20892, USA

Corresponding authors: Srinivas Vourganti. Email: vourgans@upstate.edu and Leszek Kotula. Email: kotulal@upstate.edu

Abstract

Prostate cancer is one of the most common malignancies affecting men worldwide. High mortality rates from advanced and metastatic prostate cancer in the United States are contrasted by a relatively indolent course in the majority of cases. This gives hope for finding methods that could direct personalized diagnostic, preventative, and treatment approaches to patients with prostate cancer. Recent advances in multiparametric magnetic resonance imaging (MP-MRI) offer a noninvasive diagnostic intervention which allows correlation of prostate tumor image characteristics with underlying biologic evidence of tumor progression. The power of MP-MRI includes examination of both local invasion and nodal disease and might overcome the challenges of analyzing the multifocal nature of prostate cancer. Future directions include a careful analysis of the genomic signature of individual prostatic lesions utilizing image-guided biopsies. This review examines the diagnostic potential of MRI in prostate cancer.

Keywords: Prostate cancer, magnetic resonance imaging, lymph node imaging, image-guided biopsy, radiobiology

***Experimental Biology and Medicine* 2014; 239: 805–812. DOI: 10.1177/1535370214536669**

Introduction

Adenocarcinoma of the prostate gland remains the most common solid organ malignancy in men in the United States with an estimated 233,000 new diagnoses and 29,480 deaths in 2014, representing 10% of all cancer related mortality in men.[1] Despite this high incidence, the vast majority of men identified with prostate cancer will never actually die of the disease, with approximately one in 36 men diagnosed dying of prostate specific mortality (http://www.cancer.org/cancer/prostatecancer/detailedguide/prostate-cancer-key-statistics).

Great strides have been made in improving the mortality from prostate cancer. Mortality rates fell significantly in industrialized countries which is contributed in part by the widespread application of curative treatment of patients diagnosed in the early stages of disease.[2] Unfortunately, this progress has come hand in hand with the overtreatment of many men who are likely to have never died of their prostate cancer. Distinguishing between clinically significant and indolent prostate cancers in men diagnosed in early stages of malignancy is a major focus of current inquiry. Presently established clinical paradigms utilizing serum prostate specific antigen assays and screening tools such as systematic transrectal ultrasound-guided biopsy suffer from poor sensitivity and specificity[3,4] and ultimately lead to both overdetection of low risk indolent lesions as well as missed cancers of high oncologic risk. This clinical uncertainty is reflected in the high upgrading rate between clinical predictions of cancer significance and true pathologic findings after radical prostatectomy, occurring nearly 30% of the time.[5] As a result, neither clinician nor patient can completely rely on clinical staging information to predict indolence and many men turn to invasive and radical treatment even in the setting of predicted low risk cancer.

A great deal of investigative effort has been made in improving and removing this uncertainty. Given consistent technologic improvements, it is not surprising that genomic and proteomic characterization of prostate cancer is being aggressively sought. A major limitation to the effective genomic and proteomic characterization of prostate cancer is its multifocal nature.[6] Strategies of diagnosis or treatment that ignore tumor heterogeneity will not distinguish the specific underlying genomic aberration that creates true malignant transformation as it will aggregate the results from a myriad of prostate lesions of varying risk to the patient.

Recent advances in the radiologic imaging of patients with prostate cancer, specifically those protocols which utilize 3 Tesla magnetic resonance imaging (MRI) coupled with an endorectal coil, have improved the signal-to-noise ratio of image acquisition and have achieved a revolutionary improvement in temporal and spatial resolution.[7] This imaging clarity has finally offered adequate insight into the three-dimensional anatomy of the gland to allow identification and characterization of individual prostate tumor lesions within the gland.

Moreover, by utilizing the combination of conventional anatomic MRI with advanced functional MR sequences (known as multiparametric imaging, including diffusion weighted imaging (DWI), dynamic contrast enhanced [DCE] imaging, and spectroscopy) a wealth of biophysical information can be gathered about the tissue that has finally allowed true radiologic discernment between individual prostate cancer lesions and benign areas of the prostate (Figure 1).[8,9] Initial reports at centers utilizing MRI in guiding diagnostic biopsy have shown it to be superior to established techniques of random sampling in the clinical diagnosis of disease.[10,11] In this review, we aim to describe new imaging and localization techniques available to characterize prostate cancer which will ultimately be useful in distinguishing underlying biologic behavior of individual prostate cancer lesions and aid in correlative genomic and proteomic studies.

Multiparametric magnetic resonance imaging (MP-MRI)

MP-MRI is a noninvasive imaging technique, which has superior characteristics over competing imaging such as ultrasound and computed tomography (CT). Recent technologic advancements including high field strength magnets (3 T and greater) and new magnetic coil designs (including endorectal coil and multichannel surface coils) as well as advancements in software and computational algorithms have allowed the addition of more complex functional imaging to clinical imaging. Here, we describe the four component parameters of a MP-MRI study.

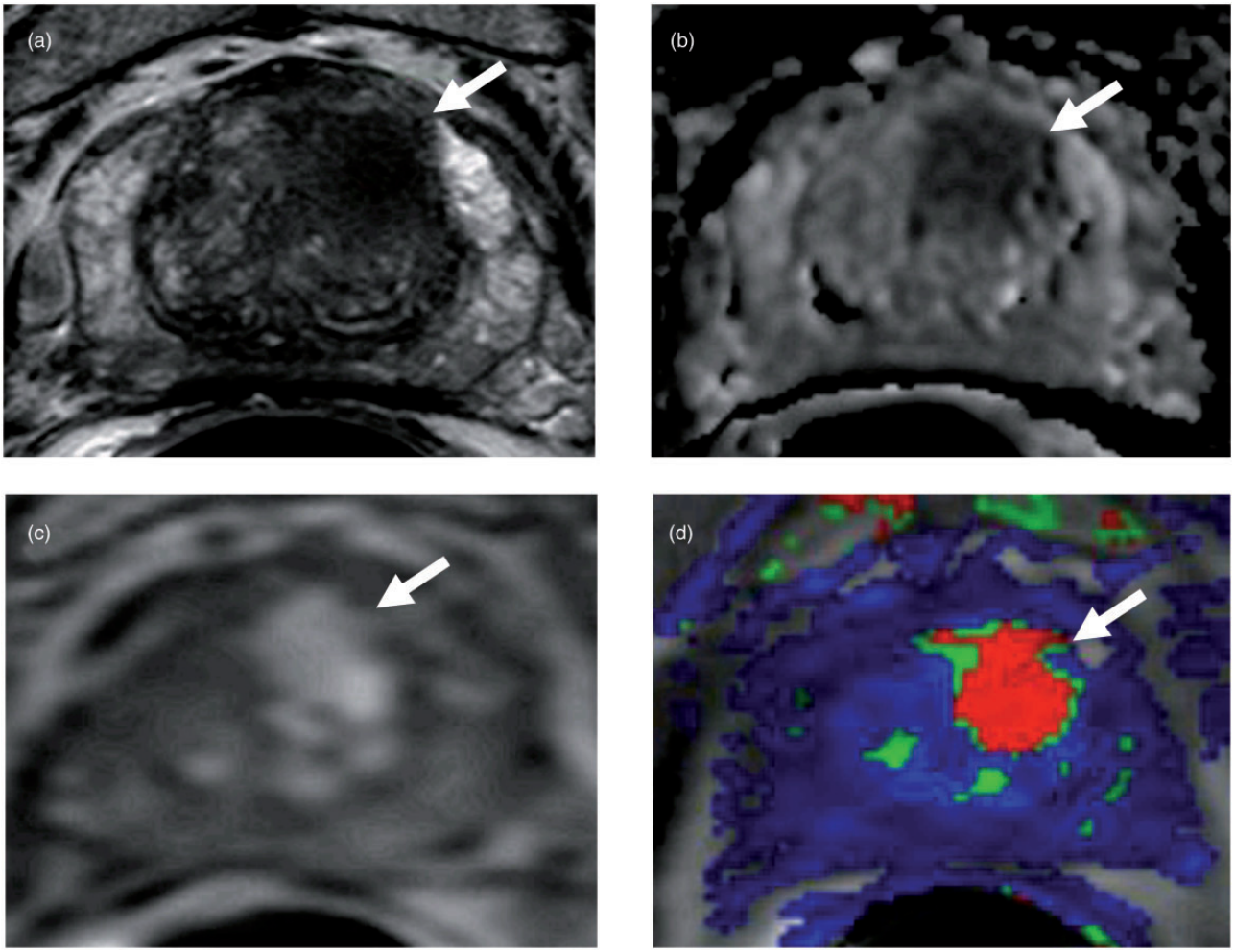

Figure 1 A 65-year-old man with a history of two prior negative TRUS-guided prostate biopsies. Axial T2W MRI shows a hypointense lesion in the left mid anterior transitional zone (arrow) (a). ADC maps of DW MRI (b), raw DCE-MRI (c), and ktrans (wash in) map of DCE-MRI (d) confirms this finding (arrows). TRUS/MRI fusion-guided biopsy revealed Gleason 3 + 4 prostate cancer within this left sided lesion

T2-weighted MRI

T2-weighted anatomic imaging is the most commonly used and widely available imaging sequence. This sequence provides excellent delineation of prostate zonal anatomy, borders, and surrounding tissues (Figure 1(a)).[8] Normal prostatic tissue exhibits relative high T2 signal intensity in the prostate peripheral zone (the origin of most adenocarcinoma lesions) and lower signal intensity in the central gland. Classically, prostate cancer lesions are noted to exhibit low signal intensity, a characteristic most easily visualized in the peripheral zone due to its normally higher signal intensity. Thus, rare transitional zone and central gland lesions are much more difficult to identify in this sequence. In addition, many benign conditions can mimic this appearance of low signal intensity (such as inflammation). As a result, when relying on only this parameter approximately half of lesions are missed.[12] Also, not surprisingly, lesion size has significant impact on detection, with larger tumors (1 cm) nearly always visualized and smaller tumors (<5 mm) much more likely missed.[13]

Owing to the detail of T2 imaging, it is the most helpful sequence for assessing local invasion into surrounding tissues. Detection of this local invasion has clinical relevance as it decreases the likelihood of cure from local therapy. Such invasion can be seen most overtly as direct invasion into the periprostatic fat. In addition, other findings suggestive of local invasion are irregularity of the gland margin, capsular bulge, and a low signal area within the seminal vesicles (which normally exhibit very high signal intensity). The results from such local staging predictions are not perfect, however, and absence of findings may occur in the setting of true disease with reports of diagnostic sensitivity ranging from 50 to 60%.[14,15]

Diffusion weighted MRI (DW-MRI)

DW-MRI sequences can detect and quantify the Brownian motion of water within tissue *in vivo*.[16] As this relates to cellular density, cell permeability, and free water diffusion within the interstitial spaces, DW-MRI can assess tissue structural architecture and differentiate benign issue from malignant tissue. Benign tissue exhibits high signal intensity as it normally allows free water to diffuse with relative ease. In the malignant setting, relatively higher nuclear:cytoplasmic ratio and loss of extracellular spaces due to cellular proliferation results in decreased free water diffusion and thus relatively lower signal intensity on DW-MRI (Figure 1(b)).[17] Furthermore, DW-MRI findings have been significantly correlated to underlying histopathologic grade and clinical risk scores,[18] which allows some prediction of tumor histopathologic behavior based on radiologic findings. Downsides of DW-MRI include its relatively poor spatial resolution (especially in comparison to T2-weighted MRI), which limits the ability to evaluate staging using this sequence in isolation. In addition, DW-MRI is more challenging to interpret in the central gland as the presence of benign hyperplastic (BPH) associated nodules in this area of the prostate can mimic the low signal intensity of malignant lesions.[19] Despite this, addition of DW-MRI to standard anatomic T2-weighted imaging has been demonstrated to improve diagnostic accuracy.[12]

Dynamic contrast-enhanced magnetic resonance imaging (DCE-MRI)

DCE-MRI allows assessment of tissue vascular supply by acquiring T1-weighted images continuously before, throughout, and continuing after the injection of an MRI detectable contrast agent (i.e. gadolinium). Signal increase during this protocol results from blood supply to the tissue of interest. Differentiation between normal and malignant tissue is possible, as cancers have a typical imaging signature owing to their disordered angiogenesis (Figure 1(c) and (d)). Malignant tissue is correlated with early uptake and early washout (temporal imaging) of vascular contrast.[20] These changes are most easily seen in larger lesions and in lesions, which are of higher grade. In addition, similar to T2-weighted and DWI-MRI, lesions in the central gland are more challenging to differentiate as BPH nodules themselves can show early uptake, though they do not classically have the rapid washout typical of malignant lesions. DCE-MRI has been shown to have higher diagnostic power than T2W sequences alone, especially in lesions larger than 5 mm.[21] Similar to DWI, DCE-MRI sequences have relatively poor spatial resolution (in comparison to T2-weighted MRI) which limits the ability to evaluate staging using this sequence in isolation. However, it is felt to be most useful in the assessment of treatment effects in settings where the prostate gland remains *in situ*.

Magnetic resonance spectroscopic imaging (MRSI)

Nuclear magnetic resonance spectroscopy(MRS) is possible *in situ* using MRSI, which allows relative quantification of metabolites within the tissue of interest. In this technique, the tissue of interest is divided into discrete areas (volumes of interest) known as voxels. For each voxel, a spectra of electromagnetic (EM) radiation is acquired which represents a fingerprint of the composition of the volume. These data can be used to differentiate benign from malignant tissue. Benign prostate cancer typically harbors high levels of citrate, which can be detected as a specific peak on MRSI spectra. In the setting of cancer, the increased cellular turnover results in a relatively high concentration of choline, also detectable on the MRSI spectral curve. From these data, the relative concentration of choline:citrate can be calculated, with increased ratios signifying malignant changes. The addition of MRSI has been shown to improve diagnostic accuracy over T2-weighted imaging alone, with especially high specificity.[22] Some challenges to this technique are that inflammation can mimic citrate:choline signal changes and that spatial resolution (similar to DWI and DCE-MRI) is not as good as T2-weighted MRI in the aid of local staging. In addition, some centers report that it is technically challenging and on some platforms it increases acquisition times limiting its widespread utilization.

MP-MRI—combining imaging parameters for improved diagnostic power

As each individual parameter is capturing orthogonal data, the combination of them has been demonstrated to have improved diagnostic power over each individual in isolation. Using careful histopathologic correlation of radical prostatectomy specimens, it has been demonstrated that a lesion identified has a positive predictive value of 98%, with excellent sensitivity especially in larger lesions of clinical significance (>5 mm).[22]

Iron oxide imaging in lymph node MRI in prostate cancer patients

In addition to local staging within and immediately around the prostate gland, accurate lymph node staging is critical for treatment planning in patients with prostate cancer, and its implication on prognosis has been well studied.[23–25] In patients with high-risk prostate cancer (prostate-specific antigen >20 ng/dL, Gleason ≥8, or extra-prostatic spread), there is a high risk of biochemical recurrence after localized treatment, eventually leading to metastasis and death.[26] The 5-year survival rates depend on the total number of metastatic lymph nodes and range from 75 to 80% in patients with a single metastatic node to only 20–30% in patients more than five metastatic nodes.[27] In most patients, the initial seeding of metastatic cells occurs in pelvic lymph nodes, so the status of the pelvic lymph nodes largely determines the appropriate management of the primary tumor.[28] Surgical pelvic lymph node dissection with histopathological examination is the most common method of assessing lymph node status; however, extended pelvic node dissection is a technically challenging surgery and is associated with higher complication rates such as lymphocele, deep venous thrombosis, pelvic hematoma, fever, and urinary retention that may result in longer hospital stays.[29] Thus, there is an urgent clinical need for a reliable preoperative imaging method demonstrating metastatic involvement of lymph nodes, which could improve the completeness of lymph node removal by targeting malignant nodes to be removed. Furthermore, by identifying metastatic lymph nodes preoperatively, imaging may help improve oncologic outcomes or render a complete lymph node dissection unnecessary when imaging shows no metastatic lymph nodes.

Current available imaging techniques for the detection of metastatic lymph nodes in patients with prostate cancer include CT and MRI of the abdomen and pelvis, which both primarily depend on size criteria to distinguish malignant nodes from benign ones. According to the response evaluation criteria in solid tumors, a lymph node is considered metastatic if the short-axis measurement is ≥1.5 cm.[30] However, the use of these criteria may result in false negatives in metastatic lymph nodes of normal size and false positives in benign enlarged lymph nodes due to inflammation or infection.[31,32] CT offers high spatial resolution and rapid image acquisition while MRI provides excellent anatomical detail and soft-tissue resolution. However, these conventional imaging methods have limited sensitivities ranging from 24 to 78% and 27 to 69% for the detection of metastatic lymph nodes.[33–40] An imaging method incorporating both anatomical and functional information for accurate imaging of pelvic lymph nodes is needed in prostate cancer treatment planning.

MR images can be improved by the use of contrast agents containing ultrasmall particles of iron oxide (USPIO), which are taken up by macrophages in lymph nodes, thus allowing visualization of early histological changes caused by infiltrating tumor cells, even before the lymph nodes have enlarged.[41] The USPIO agent is injected intravenously and then passes through capillary walls and is taken up by the reticuloendothelial system allowing particles to drain into lymph nodes.[42] Within normal lymph nodes, the USPIO agent is internalized by macrophages and accumulates within the node, causing a signal drop on T2 MR images, whereas lymph nodes with metastatic involvement retain their preenhancement signal characteristics.[43,44] Several studies have shown the utility of lymph node MR imaging using USPIO agents in patients with prostate cancer. Harisinghani *et al.* reported the usefulness of USPIO-enhanced MRI in the detection of small lymph node metastases in 33 patients with prostate cancer using the USPIO particle ferumoxtran-10.[41] Heesakkers *et al.* compared image quality of USPIO (ferumoxtran-10) enhanced MRI with 1.5 T and 3 T systems in 48 patients with prostate cancer and concluded that 3 T systems provide improved image quality and lymph node border delineation.[45] The same group also recently showed the utility of USPIO enhanced MRI for the detection of lymph node metastases outside the area of routine pelvic lymph node dissection in 41% of 58 patients with prostate cancer.[46]

USPIO-enhanced MRI has several limitations, including the need to perform imaging precontrast and 24–36 h post-contrast due to the slow accumulation of the contrast agent within lymph nodes. Furthermore, the USPIO agent ferumoxtran-10 has been studied by many groups but requires slow administration through a filtered needle over 15–30 min to minimize hypersensitivity reactions. Though available for use in research settings, it is not currently available for clinical use in the United States and Europe. Further studies examining the use of USPIO-enhanced MRI in lymph node imaging are needed.

Harnessing MRI data: Capturing lesion-specific tissue samples

Once this detailed mapping of the prostate and its inclusive tumors is completed, a second more challenging issue arises of how to reach this tissue and isolate it specific to prostate lesional anatomy. New strides in this effort have been aided by technological advancements in on-demand additive manufacturing (3D-printed) molds of a patient's prostate gland (based on segmentation data from T2-weighted anatomic data).[22] By utilizing a computer aided prostate segmentation algorithm, and aided by manual corrections by a trained prostate radiologist, the boundaries of the prostate can be mapped and a digital 3D solid object model can be calculated from the patients' MRI imaging data. This 3D solid object data can then be used to make a patient-specific

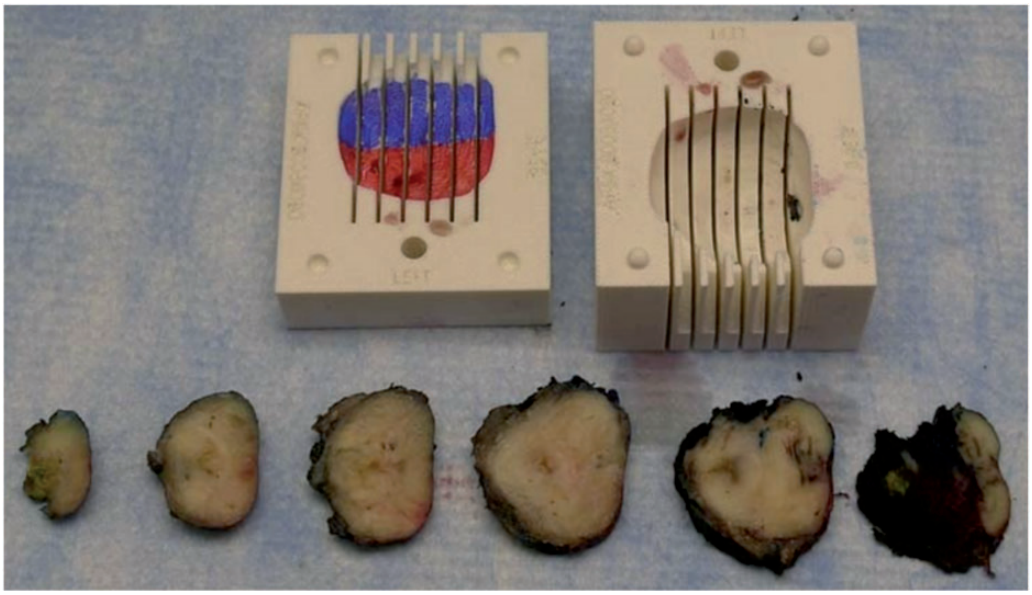

Figure 2 A customized mold is fabricated using three-dimensional segmentation data from the MRI scan. Grooves are placed in the mold, which specifically correspond to the location of the MRI slices throughout the prostate gland aiding whole mount sectioning. In this way, gross pathology specimens can be carefully correlated to MRI imaging data

mold which is personalized to the exact anatomy of the patient. The mold is designed with specifically placed grooves which correspond to the MRI slice levels. In this way, the gross anatomic pathologist can make a cut which exactly corresponds (with six axis accuracy) to the MRI imaging slice (Figure 2). These efforts have allowed precise 1:1 correspondence between MRI data and histopathology. This advance has allowed for the publication of numerous reports which demonstrate excellent correlation of MR and histopathology.[8,22,47]

If the whole gland is not available (on autopsy or following radical prostatectomy), there are additional MRI-guided biopsy approaches newly available. These effectively allow *in situ* lesion-specific sampling utilizing transperineal or transrectal biopsy. New breakthroughs using fusion ultrasound/MRI have even allowed this MRI-guided lesional specific tissue sampling to be performed on an outpatient basis on a patient using local anesthesia only.[48]

Can characteristics of MRI lesions be diagnostic?—Defining the genomic signature of MRI lesions associated with aggressive prostate cancer

Correlation of physical features of MRI-identified lesion with specific genetic signatures will aid in evaluation of diagnostic potential of MP-MRI. Using genome-wide analysis of exome- and gene-specific mutation, as well as copy number variations (CNV) and methylation studies, changes specific to each lesion can be identified as compared to healthy prostate tissue. These genomic changes may parallel findings on MP-MRI. The size of the tumor lesion, characterized by T2 weighted imaging, may be correlated with TMPRSS:ERG, AR, and PTEN mutations, as well as key changes in methylation.[49,50] Disordering of the tissue, characterized by DWI, may be correlated with BRCA2 and TP53 deficiency,[51] or WNT16B mutations,[52] as well as tumor-specific methylation changes[53] and/or CNV variations.[54] Disruptions in angiogenesis, characterized by DCE imaging, may be correlated with mutations in vascular endothelial factor (VEGF) family, hypoxia-inducible factor (HIF) family, mTOR and PTEN mutations. Finally, altered metabolic activity in the tissue, characterized by MRS, may be correlated with TP53, Rb, and PTEN mutations, as alterations in these genes can lead to increased cell turnover.[55] By using these key mutations to create a genetic signature for an MRI lesion, genomic analysis can provide important prognostic information regarding tumor progression.

Prostate tumor progression can be modeled *in vivo* in the mouse

Mice have proven to be quite important for better understanding of prostate cancer initiation and tumor progression mechanisms as well as tumor sensitivities to investigational drugs.[56–58] Low incidence of prostate pathology in the mouse[59,60] and knowledge of mouse genetics and availability of genetically engineered mouse model strains for several tumor drivers, and availability of probasin-driven Cre strain[61] permitted modeling of the loss of heterozygosity hypothesis in the mouse. Use of Nkx3.1 promoter driven Cre may allow better targeting of genetic inactivation in the luminal epithelium.[62] Simultaneous use of the frt-mediated deletion[63] and Cre recombination might expand the possibilities of genetic targeting in the mouse to include time-controlled or sequential inactivation of genes. Blueprint for translational use of mice in cancer has been demonstrated for acute promyelocytic leukemia (APL)[64] and now it is applied for prostate cancer[65] and other types of cancer.[66]

Key drivers of prostate tumorigenesis in the human also induce pathology in the mouse. These include TP53,

c-MYC, TMPRSS2-ERG rearrangements, RB, and PTEN. Modeling Pten as a second hit to disruption of the gene that initiates PIN modulates prostate tumor progression in the mouse such as Nkx3.1[67] or PI3 kinase.[68] New developments in mouse prostate cancer modeling include lymph node metastasis model[69] and conditional knockout of the adaptor protein Abi1 that produces PIN due to actin cytoskeleton dysregulation.[70] Phenotypic signatures of genetic interactions of two or more genes may be potentially evaluated by MRI[65,71] to model physical changes observed in human patients.

Conclusion

The advancement of prostate cancer treatment will ultimately require a better understanding of underlying tumor biology. As a heterogeneous, multifocal disease with widely varying behavior, it is imperative to identify specific underlying predictive factors which can more accurately guide therapy decisions. Recent advances in imaging have allowed for specific radiologic characterization of primary lesions as well as nodal and distant foci of disease. By harnessing this information and combining it with *in vitro* and genomic characterization, great strides in our understanding of prostate cancer behavior can be made.

Author contribution: SV and LK conceived the idea for the review. SV, JD, LJ, BT, GB, and LK wrote the manuscript. Authors declare no conflict of interest.

ACKNOWLEDGEMENTS

This work was supported in part by the grant from National Cancer Institute (LK) R01CA161018.

REFERENCES

1. Siegel R, Ma J, Zou Z, Jemal A. Cancer statistics, 2014. *CA Cancer J Clin* 2014;**64**:9–29
2. Jemal A, Bray F, Center MM, Ferlay J, Ward E, Forman D. Global cancer statistics. *CA Cancer J Clin* 2011;**61**:69–90
3. Ouzaid I, Yates DR, Hupertan V, Mozer P, Chartier-Kastler E, Haertig A, Bitker MO, Roupret M. A direct comparison of the diagnostic accuracy of three prostate cancer nomograms designed to predict the likelihood of a positive initial transrectal biopsy. *Prostate* 2012;**72**:1200–6
4. Haas GP, Delongchamps NB, Jones RF, Chandan V, Serio AM, Vickers AJ, Jumbelic M, Threatte G, Korets R, Lilja H, de la Roza G. Needle biopsies on autopsy prostates: Sensitivity of cancer detection based on true prevalence. *J Natl Cancer Inst* 2007;**99**:1484–9
5. Tilki D, Schlenker B, John M, Buchner A, Stanislaus P, Gratzke C, Karl A, Tan GY, Ergun S, Tewari AK, Stief CG, Seitz M, Reich O. Clinical and pathologic predictors of Gleason sum upgrading in patients after radical prostatectomy: Results from a single institution series. *Urol Oncol* 2011;**29**:508–14
6. Andreoiu M, Cheng L. Multifocal prostate cancer: Biologic, prognostic, and therapeutic implications. *Hum Pathol* 2010;**41**:781–93
7. Lagemaat MW, Scheenen TW. Role of high-field MR in studies of localized prostate cancer. *NMR Biomed* 2014;**27**:67–79
8. Turkbey B, Pinto PA, Mani H, Bernardo M, Pang Y, McKinney YL, Khurana K, Ravizzini GC, Albert PS, Merino MJ, Choyke PL. Prostate cancer: Value of multiparametric MR imaging at 3 T for detection—histopathologic correlation. *Radiology* 2010;**255**:89–99
9. Panebianco V, Sciarra A, Marcantonio A, Forte V, Biondi T, Laghi A, Catalano C. Conventional imaging and multiparametric magnetic resonance (MRI, MRS, DWI, MRP) in the diagnosis of prostate cancer. *Q J Nucl Med Mol Imaging* 2012;**56**:331–42
10. Pinto PA, Chung PH, Rastinehad AR, Baccala AA Jr., Kruecker J, Benjamin CJ, Xu S, Yan P, Kadoury S, Chua C, Locklin JK, Turkbey B, Shih JH, Gates SP, Buckner C, Bratslavsky G, Linehan WM, Glossop ND, Choyke PL, Wood BJ. Magnetic resonance imaging/ultrasound fusion guided prostate biopsy improves cancer detection following transrectal ultrasound biopsy and correlates with multiparametric magnetic resonance imaging. *J Urol* 2011;**186**:1281–5
11. Vourganti S, Rastinehad A, Yerram NK, Nix J, Volkin D, Hoang A, Turkbey B, Gupta GN, Kruecker J, Linehan WM, Choyke PL, Wood BJ, Pinto PA. Multiparametric magnetic resonance imaging and ultrasound fusion biopsy detect prostate cancer in patients with prior negative transrectal ultrasound biopsies. *J Urol* 2012;**188**:2152–7
12. Haider MA, van der Kwast TH, Tanguay J, Evans AJ, Hashmi AT, Lockwood G, Trachtenberg J. Combined T2-weighted and diffusion-weighted MRI for localization of prostate cancer. *AJR Am J Roentgenol* 2007;**189**:323–8
13. Nakashima J, Tanimoto A, Imai Y, Mukai M, Horiguchi Y, Nakagawa K, Oya M, Ohigashi T, Marumo K, Murai M. Endorectal MRI for prediction of tumor site, tumor size, and local extension of prostate cancer. *Urology* 2004;**64**:101–5
14. Park BK, Kim B, Kim CK, Lee HM, Kwon GY. Comparison of phased-array 3.0-T and endorectal 1.5-T magnetic resonance imaging in the evaluation of local staging accuracy for prostate cancer. *J Comput Assist Tomogr* 2007;**31**:534–8
15. Futterer JJ, Engelbrecht MR, Huisman HJ, Jager GJ, Hulsbergen-van De Kaa CA, Witjes JA, Barentsz JO. Staging prostate cancer with dynamic contrast-enhanced endorectal MR imaging prior to radical prostatectomy: Experienced versus less experienced readers. *Radiology* 2005;**237**:541–9
16. Issa B. In vivo measurement of the apparent diffusion coefficient in normal and malignant prostatic tissues using echo-planar imaging. *J Magn Reson Imaging* 2002;**16**:196–200
17. Lim KS, Tan CH. Diffusion-weighted MRI of adult male pelvic cancers. *Clin Radiol* 2012;**67**:899–908
18. Turkbey B, Shah VP, Pang Y, Bernardo M, Xu S, Kruecker J, Locklin J, Baccala AA Jr., Rastinehad AR, Merino MJ, Shih JH, Wood BJ, Pinto PA, Choyke PL. Is apparent diffusion coefficient associated with clinical risk scores for prostate cancers that are visible on 3-T MR images? *Radiology* 2011;**258**:488–95
19. Oto A, Kayhan A, Jiang Y, Tretiakova M, Yang C, Antic T, Dahi F, Shalhav AL, Karczmar G, Stadler WM. Prostate cancer: Differentiation of central gland cancer from benign prostatic hyperplasia by using diffusion-weighted and dynamic contrast-enhanced MR imaging. *Radiology* 2010;**257**:715–23
20. Verma S, Turkbey B, Muradyan N, Rajesh A, Cornud F, Haider MA, Choyke PL, Harisinghani M. Overview of dynamic contrast-enhanced MRI in prostate cancer diagnosis and management. *Am J Roentgenol* 2012;**198**:1277–88
21. Puech P, Potiron E, Lemaitre L, Leroy X, Haber GP, Crouzet S, Kamoi K, Villers A. Dynamic contrast-enhanced-magnetic resonance imaging evaluation of intraprostatic prostate cancer: Correlation with radical prostatectomy specimens. *Urology* 2009;**74**:1094–9
22. Turkbey B, Mani H, Shah V, Rastinehad AR, Bernardo M, Pohida T, Pang Y, Daar D, Benjamin C, McKinney YL, Trivedi H, Chua C, Bratslavsky G, Shih JH, Linehan WM, Merino MJ, Choyke PL, Pinto PA. Multiparametric 3T prostate magnetic resonance imaging to detect cancer: Histopathological correlation using prostatectomy specimens processed in customized magnetic resonance imaging based molds. *J Urol* 2011;**186**:1818–24
23. Bader P, Burkhard FC, Markwalder R, Studer UE. Disease progression and survival of patients with positive lymph nodes after radical prostatectomy Is there a chance of cure?. *J Urol* 2003;**169**:849–54
24. Cheng L, Bergstralh EJ, Cheville JC, Slezak J, Corica FA, Zincke H, Blute ML, Bostwick DG. Cancer volume of lymph node metastasis

predicts progression in prostate cancer. *Am J Surg Pathol* 1998;**22**:1491–1500
25. Kothari PS, Scardino PT, Ohori M, Kattan MW, Wheeler TM. Incidence, location, and significance of periprostatic and periseminal vesicle lymph nodes in prostate cancer. *Am J Surg Pathol* 2001;**25**:1429–32
26. Bastian PJ, Boorjian SA, Bossi A, Briganti A, Heidenreich A, Freedland SJ, Montorsi F, Roach M 3rd, Schroder F, van Poppel H, Stief CG, Stephenson AJ, Zelefsky MJ. High-risk prostate cancer: From definition to contemporary management. *Eur Urol* 2012;**61**:1096–106
27. Daneshmand S, Quek ML, Stein JP, Lieskovsky G, Cai J, Pinski J, Skinner EC, Skinner DG. Prognosis of patients with lymph node positive prostate cancer following radical prostatectomy: Long-term results. *J Urol* 2004;**172**:2252–5
28. Hansen J, Rink M, Bianchi M, Kluth LA, Tian Z, Ahyai SA, Shariat SF, Briganti A, Steuber T, Fisch M, Graefen M, Karakiewicz PI, Chun FK. External validation of the updated Briganti nomogram to predict lymph node invasion in prostate cancer patients undergoing extended lymph node dissection. *Prostate* 2013;**73**:211–8
29. Briganti A, Chun FK, Salonia A, Suardi N, Gallina A, Da Pozzo LF, Roscigno M, Zanni G, Valiquette L, Rigatti P, Montorsi F, Karakiewicz PI. Complications and other surgical outcomes associated with extended pelvic lymphadenectomy in men with localized prostate cancer. *Eur Urol* 2006;**50**:1006–13
30. Chalian H, Tore HG, Horowitz JM, Salem R, Miller FH, Yaghmai V. Radiologic assessment of response to therapy: Comparison of RECIST Versions 1.1 and 1.0. *Radiographics* 2011;**31**:2093–105
31. Campbell SC, Klein EA, Levin HS, Piedmonte MR. Open pelvic lymph node dissection for prostate cancer: A reassessment. *Urology* 1995;**46**:352–5
32. Tiguert R, Gheiler EL, Tefilli MV, Oskanian P, Banerjee M, Grignon DJ, Sakr W, Pontes JE, Wood DP Jr. Lymph node size does not correlate with the presence of prostate cancer metastasis. *Urology* 1999;**53**:367–71
33. Tempany CM, McNeil BJ. Advances in biomedical imaging. *JAMA* 2001;**285**:562–7
34. Bott SR. Management of recurrent disease after radical prostatectomy. *Prostate Cancer Prostatic Dis* 2004;**7**:211–6
35. Kane CJ, Amling CL, Johnstone PA, Pak N, Lance RS, Thrasher JB, Foley JP, Riffenburgh RH, Moul JW. Limited value of bone scintigraphy and computed tomography in assessing biochemical failure after radical prostatectomy. *Urology* 2003;**61**:607–11
36. Bezzi M, Kressel HY, Allen KS, Schiebler ML, Altman HG, Wein AJ, Pollack HM. Prostatic carcinoma: Staging with MR imaging at 1.5 T. *Radiology* 1988;**169**:339–46
37. Borley N, Fabrin K, Sriprasad S, Mondaini N, Thompson P, Muir G, Poulsen J. Laparoscopic pelvic lymph node dissection allows significantly more accurate staging in ''high-risk'' prostate cancer compared to MRI or CT. *Scand J Urol Nephrol* 2003;**37**:382–6
38. Jager GJ, Barentsz JO, Oosterhof GO, Witjes JA, Ruijs SJ. Pelvic adenopathy in prostatic and urinary bladder carcinoma: MR imaging with a three-dimensional TI-weighted magnetization-prepared-rapid gradient-echo sequence. *Am J Roentgenol* 1996;**167**:1503–7
39. Oyen RH, Van Poppel HP, Ameye FE, Van de Voorde WA, Baert AL, Baert LV. Lymph node staging of localized prostatic carcinoma with CT and CT-guided fine-needle aspiration biopsy: Prospective study of 285 patients. *Radiology* 1994;**190**:315–22
40. Wang L, Hricak H, Kattan MW, Schwartz LH, Eberhardt SC, Chen HN, Scardino PT. Combined endorectal and phased-array MRI in the prediction of pelvic lymph node metastasis in prostate cancer. *Am J Roentgenol* 2006;**186**:743–8
41. Harisinghani MG, Barentsz J, Hahn PF, Deserno WM, Tabatabaei S, van de Kaa CH, de la Rosette J, Weissleder R. Noninvasive detection of clinically occult lymph-node metastases in prostate cancer. *N Engl J Med* 2003;**348**:2491–9
42. Wang YX, Hussain SM, Krestin GP. Superparamagnetic iron oxide contrast agents: Physicochemical characteristics and applications in MR imaging. *Eur Radiol* 2001;**11**:2319–31
43. Weissleder R, Elizondo G, Wittenberg J, Rabito CA, Bengele HH, Josephson L. Ultrasmall superparamagnetic iron oxide: Characterization of a new class of contrast agents for MR imaging. *Radiology* 1990;**175**:489–93
44. Wunderbaldinger P, Josephson L, Bremer C, Moore A, Weissleder R. Detection of lymph node metastases by contrast-enhanced MRI in an experimental model. *Magn Reson Med* 2002;**47**:292–7
45. Heesakkers RA, Futterer JJ, Hovels AM, van den Bosch HC, Scheenen TW, Hoogeveen YL, Barentsz JO. Prostate cancer evaluated with ferumoxtran-10-enhanced T2*-weighted MR Imaging at 1.5 and 3.0 T: Early experience. *Radiology* 2006;**239**:481–7
46. Heesakkers RA, Jager GJ, Hovels AM, de Hoop B, van den Bosch HC, Raat F, Witjes JA, Mulders PF, van der Kaa CH, Barentsz JO. Prostate cancer: Detection of lymph node metastases outside the routine surgical area with ferumoxtran-10-enhanced MR imaging. *Radiology* 2009;**251**:408–14
47. Trivedi H, Turkbey B, Rastinehad AR, Benjamin CJ, Bernardo M, Pohida T, Shah V, Merino MJ, Wood BJ, Linehan WM, Venkatesan AM, Choyke PL, Pinto PA. Use of patient-specific MRI-based prostate mold for validation of multiparametric MRI in localization of prostate cancer. *Urology* 2012;**79**:233–9
48. Logan JK, Rais-Bahrami S, Turkbey B, Gomella A, Amalou H, Choyke PL, Wood BJ, Pinto PA. Current Status of MRI and ultrasound fusion software platforms for guidance of prostate biopsies. *BJU Int* 2013; (epub ahead of print)
49. Yu J, Yu J, Mani RS, Cao Q, Brenner CJ, Cao X, Wang X, Wu L, Li J, Hu M, Gong Y, Cheng H, Laxman B, Vellaichamy A, Shankar S, Li Y, Dhanasekaran SM, Morey R, Barrette T, Lonigro RJ, Tomlins SA, Varambally S, Qin ZS, Chinnaiyan AM. An integrated network of androgen receptor, polycomb, and TMPRSS2-ERG gene fusions in prostate cancer progression. *Cancer Cell* 2010;**17**:443–54
50. Berger MF, Lawrence MS, Demichelis F, Drier Y, Cibulskis K, Sivachenko AY, Sboner A, Esgueva R, Pflueger D, Sougnez C, Onofrio R, Carter SL, Park K, Habegger L, Ambrogio L, Fennell T, Parkin M, Saksena G, Voet D, Ramos AH, Pugh TJ, Wilkinson J, Fisher S, Winckler W, Mahan S, Ardlie K, Baldwin J, Simons JW, Kitabayashi N, MacDonald TY, Kantoff PW, Chin L, Gabriel SB, Gerstein MB, Golub TR, Meyerson M, Tewari A, Lander ES, Getz G, Rubin MA, Garraway LA. The genomic complexity of primary human prostate cancer. *Nature* 2011;**470**:214–20
51. Francis JC, McCarthy A, Thomsen MK, Ashworth A, Swain A. Brca2 and Trp53 deficiency cooperate in the progression of mouse prostate tumourigenesis. *PLoS Genet* 2010;**6**:e1000995
52. Sun Y, Campisi J, Higano C, Beer TM, Porter P, Coleman I, True L, Nelson PS. Treatment-induced damage to the tumor microenvironment promotes prostate cancer therapy resistance through WNT16B. *Nat Med* 2012;**18**:1359–68
53. Kobayashi Y, Absher DM, Gulzar ZG, Young SR, McKenney JK, Peehl DM, Brooks JD, Myers RM, Sherlock G. DNA methylation profiling reveals novel biomarkers and important roles for DNA methyltransferases in prostate cancer. *Genome Res* 2011;**21**:1017–27
54. Jin G, Sun J, Liu W, Zhang Z, Chu LW, Kim ST, Sun J, Feng J, Duggan D, Carpten JD, Wiklund F, Gronberg H, Isaacs WB, Zheng SL, Xu J. Genome-wide copy-number variation analysis identifies common genetic variants at 20p13 associated with aggressiveness of prostate cancer. *Carcinogenesis* 2011;**32**:1057–62
55. Cairns RA, Harris IS, Mak TW. Regulation of cancer cell metabolism. *Nat Rev Cancer* 2011;**11**:85–95
56. Abate-Shen C. A new generation of mouse models of cancer for translational research. *Clin Cancer Res* 2006;**12**:5274–6
57. Abate-Shen C, Pandolfi PP. Effective utilization and appropriate selection of genetically engineered mouse models for translational integration of mouse and human trials. *Cold Spring Harb Protocols* 2013;**2013**:1006–11
58. Grabowska MM, Degraff DJ, Yu X, Jin RJ, Chen Z, Borowsky AD, Matusik RJ. Mouse models of prostate cancer: Picking the best model for the question. *Cancer Metastasis Rev* 2014; (epub ahead of print)
59. Suwa T, Nyska A, Haseman JK, Mahler JF, Maronpot RR. Spontaneous lesions in control B6C3F1 mice and recommended sectioning of male accessory sex organs. *Toxicol Pathol* 2002;**30**:228–34

60. Shappell SB, Thomas GV, Roberts RL, Herbert R, Ittmann MM, Rubin MA, Humphrey PA, Sundberg JP, Rozengurt N, Barrios R, Ward JM, Cardiff RD. Prostate pathology of genetically engineered mice: Definitions and classification. The consensus report from the Bar Harbor meeting of the Mouse Models of Human Cancer Consortium Prostate Pathology Committee. *Cancer Res* 2004;**64**:2270–2305
61. Wu X, Wu J, Huang J, Powell WC, Zhang J, Matusik RJ, Sangiorgi FO, Maxson RE, Sucov HM, Roy-Burman P. Generation of a prostate epithelial cell-specific Cre transgenic mouse model for tissue-specific gene ablation. *Mech Dev* 2001;**101**:61–69
62. Wang X, Kruithof-de Julio M, Economides KD, Walker D, Yu H, Halili MV, Hu YP, Price SM, Abate-Shen C, Shen MM. A luminal epithelial stem cell that is a cell of origin for prostate cancer. *Nature* 2009;**461**:495–500
63. Rodriguez CI, Buchholz F, Galloway J, Sequerra R, Kasper J, Ayala R, Stewart AF, Dymecki SM. High-efficiency deleter mice show that FLPe is an alternative to Cre-loxP. *Nat Genet* 2000;**25**:139–40
64. Nardella C, Lunardi A, Patnaik A, Cantley LC, Pandolfi PP. The APL paradigm and the ''co-clinical trial'' project. *Cancer Discov* 2011;**1**:108–16
65. Lunardi A, Ala U, Epping MT, Salmena L, Clohessy JG, Webster KA, Wang G, Mazzucchelli R, Bianconi M, Stack EC, Lis R, Patnaik A, Cantley LC, Bubley G, Cordon-Cardo C, Gerald WL, Montironi R, Signoretti S, Loda M, Nardella C, Pandolfi PP. A co-clinical approach identifies mechanisms and potential therapies for androgen deprivation resistance in prostate cancer. *Nat Genet* 2013;**45**:747–55
66. Lunardi A, Nardella C, Clohessy JG, Pandolfi PP. Of model pets and cancer models: An introduction to mouse models of cancer. *Cold Spring Harb Protocols* 2014;**2014**:17–31
67. Abate-Shen C, Banach-Petrosky WA, Sun X, Economides KD, Desai N, Gregg JP, Borowsky AD, Cardiff RD, Shen MM. Nkx3.1; Pten mutant mice develop invasive prostate adenocarcinoma and lymph node metastases. *Cancer Res* 2003;**63**:3886–90
68. Liu P, Cheng H, Roberts TM, Zhao JJ. Targeting the phosphoinositide 3-kinase pathway in cancer. *Nat Rev Drug Discov* 2009;**8**:627–44
69. Ko HK, Akakura S, Peresie J, Goodrich DW, Foster BA, Gelman IH. A transgenic mouse model for early prostate metastasis to lymph nodes. *Cancer Res* 2014;**74**:945–53
70. Xiong X, Chorzalska A, Dubielecka PM, White JR, Vedvyas Y, Hedvat CV, Haimovitz-Friedman A, Koutcher JA, Reimand J, Bader GD, Sawicki JA, Kotula L. Disruption of Abi1/Hssh3bp1 expression induces prostatic intraepithelial neoplasia in the conditional Abi1/Hssh3bp1 KO mice. *Oncogenesis* 2012;**1**:e26
71. Trotman LC, Niki M, Dotan ZA, Koutcher JA, Di Cristofano A, Xiao A, Khoo AS, Roy-Burman P, Greenberg NM, Van Dyke T, Cordon-Cardo C, Pandolfi PP. Pten dose dictates cancer progression in the prostate. *PLoS Biol* 2003;**1**:E59